Microchemical Journal 197 (2024) 109889

Contents lists available at ScienceDirect

Microchemical Journal

journal homepage: www.elsevier.com/locate/microc

An electrochemical DNA biosensor coupled with dual amplification strategy based on DNA-Au bio-bar codes and silver enhancement for highly sensitive and selective detection of MDR1 gene

Yan Hu [a], Quan-Yu Liu [b], Xi Lin [a], Xin-Hua Lin [c,*], Hua-Ping Peng [c,*], Ai-Lin Liu [c,*]

[a] Public Technology Service Center, Fujian Medical University, Fuzhou 350122, China
[b] Department of Pharmacy, Fujian Health College, Fuzhou 350101, China
[c] The School of Pharmacy, Fujian Medical University, Fuzhou 350122, China

ARTICLE INFO

Keywords:
Dual signal amplification
DNA-Au bio-bar codes
Silver enhancement
MDR1 gene
Electrochemical DNA biosensor

ABSTRACT

Given the tumors might develop multidrug resistance (MDR) during chemotherapy that leading to treatment failure, rapid and sensitive determination of MDR1 gene is an effective tool to monitor the development of MDR. Herein, we established an electrochemical deoxyribonucleic acid (DNA) biosensor coupled with dual amplification strategy based on DNA-Au bio-bar codes and enhancement of silver for sensitive and selective determination of MDR1 gene. Specifically, DNA-Au bio-bar codes as signal probe were prepared by immobilizing complementary and non-complementary sequences on gold nanoparticles (AuNPs), so as to reduce the cross reaction between the target and reporter DNA. In addition, AuNPs-catalyzed reduction of silver ions greatly amplified the current signal. Under the optimal conditions, the current signal was proportional to the base-10 logarithm of target DNA concentration in a wide range from 100 fM to 1 nM with a detection limit as low as 33 fM (S/N = 3). Moreover, without the need for target amplification, the prepared biosensor exhibited superior selectivity and high sensitivity even in the presence of other sequences. Therefore, the developed electrochemical DNA biosensor is a facile and sensitive platform for MDR1 gene detection.

1. Introduction

Cancer is one of the most serious threats to human health and has been a leading cause of death in the world [1]. Due to the cost of treatment and the development of chemotherapy drugs, patients tend to choose chemotherapy to treat most types of cancers [2–4]. However, the development of drug resistance is one of the important reasons for chemotherapy failure in cancer [5]. When multidrug resistance (MDR) is present, the disease will progress even if chemotherapy is continued or takes other structurally unrelated drugs [6]. In general, MDR is associated with the emergence of a kind of membrane-bound glycoprotein called P-glycoprotein (P-gp). In humans, there exist two genes, i.e. MDR1 and MDR3, coding for P-gp, but only MDR1-encoded P-gp is the drug efflux protein related to MDR as defined by transfection experiments [7]. Studies revealed that the P-gp/MDR1 expression level is upregulated in cancer cells in response to the chemotherapeutic agents [8], and MDR1 gene expression level may be an useful prognostic indicator for the development of MDR during chemotherapy [9]. Currently, a variety of techniques have been developed for the detection of MDR1 gene in cancer, such as polymerase chain reaction (PCR), quantitative real-time PCR (qPCR), southern blotting, DNA sequencing and so on [10,11]. Among them, PCR is one of the most common methods, and qPCR is the gold standard for the quantitative analysis of DNA [12]. Despite this, there are unavoidable shortcomings, such as complicated operation, device requirements and incompatibility for on-site analysis [13]. Thus, it is urgently needed to develop a rapid diagnostic tool for MDR1 gene with good sensitivity and specificity.

Electrochemical DNA biosensor is a novel gene detection technology in biochemical analysis. For its merits of high sensitivity, good selectivity, rapid response, easy operation and low cost [14–17], electrochemical DNA biosensor is widely used in scientific research and clinical medicine [18–20]. Nevertheless, the ultralow abundance of target DNA accompanied with other non-specific or interference sequences in real samples still imposes restriction on the sensitivity and selectivity of the biosensor, giving rise to false-negative results [21]. Signal amplification is the most popular strategy that has been used for the ultrasensitive

* Corresponding authors.
E-mail addresses: xhl1963@sina.com (X.-H. Lin), penghuaping@fjmu.edu.cn (H.-P. Peng), ailinliu@fjmu.edu.cn (A.-L. Liu).

https://doi.org/10.1016/j.microc.2024.109889
Received 13 October 2023; Received in revised form 11 December 2023; Accepted 31 December 2023
Available online 3 January 2024
0026-265X/© 2024 Elsevier B.V. All rights reserved.

detection of DNA hybridization. Most of the signal amplification methods employ enzyme-linked signal amplification on nanocarriers to enhance the enzymatically catalytic signal. However, the practical application are limited due to the denaturation and leakage of enzymes, and the time-consuming and costly preparation and purification process [22]. Au nanoparticles (AuNPs) have been of special interest in biosensors for DNA detection due to their excellent electrical conductivity, good biocompatibility, efficient catalytic performance, low toxicity, simple preparation process and so on [23–26]. AuNPs can link with DNA via Au-N or Au-S bonds, so they are commonly used in fabrication of biosensor or DNA carrier. DNA-Au bio-bar codes, firstly proposed by Mirkin and co-workers, referred to AuNPs assembling with numerous DNA strands (the bar codes) and a corresponding recognition agent [27,28]. Due to their inherent signal amplification ability, DNA-Au bio-bar codes-based detection can realize good sensitivity, which is comparable to that of PCR without a need for target amplification [29–31]. Additionally, silver nanoparticles (AgNPs), as another nanomaterial for signal amplification, can greatly amplify the hybridization signal and can be quantitatively analyzed. Enhancement of AgNPs has good potential for biosensor applications and some novel designs have been explored in electrochemical biosensors construction based on this signal amplification method [32,33]. Letsinger *et al.* exploited a convenient and label-free approach coupled with a signal amplification tactic that deposition of AgNPs on AuNPs, which not only achieved the significant enhancement of hybridization signal, but also enlarged signal without leakage [34]. Its mechanism was that under the action of reducing agent such as hydroquinone (HQ), the silver ion reduction to AgNPs were deposited on AuNPs, while AuNPs worked as catalyst during the hybridization process. This technology was applied to DNA biosensors to attain extremely high level of sensitivity.

As mentioned above, an electrochemical DNA biosensor equipped with a dual signal amplification tactic was designed for ultrasensitive determination of MDR1. The fabrication and detection processes of the developed biosensor was illustrated in Scheme 1. Specifically, complementary and non-complementary sequences were loaded on AuNPs via Au-S bond to obtain DNA-Au bio-bar codes. Then capture probe was fixed to the glassy carbon electrode (GCE) surface by covalent coupling activator technology, and a sandwich-type DNA hybridization mode was structured. The DNA hybridization signals were significantly amplified owing to large specific surface area, excellent conductivity, fast charge transport of AuNPs and AgNPs, accompanied by the contribution of DNA-Au bio-bar codes in low cross reaction between the target and reporter sequences on the same AuNPs, thus a highly sensitive DNA biosensor was constructed for detection of MDR1. Furthermore, the developed biosensor could directly detect the target DNA in the case of interference from other biological samples. Given its high sensitivity, excellent specificity and rapid response, the developed biosensor is expected to contribute to clinical research on MDR1 gene and drug resistance progression in various diseases.

2. Experimental

2.1. Material and apparatus

1-ethyl-3-(3-dimethylammoniumpropyl)-carbamoyldiimide (EDC), silver enhancer kit, *N*-hydroxysuccinimide (NHS) and tris (2-carboxyethyl) phosphine (TCEP) were purchased from Sigma-Aldrich Co., U.S.A. Chloroauric acid ($HAuCl_4{\cdot}4H_2O$), trisodium citrate and tannic acid were obtained from Sinopharm Chemical Reagent Co., China. All oligonucleotides (Table 1) were synthesized and purified by TaKaRa Inc., China. The buffer solutions used in this study were as follows: DNA immobilization buffer (tris-ethylenediaminetetraacetic acid buffer, TE) contained 10 mM Tris-HCl, 1 mM ethylene diamine tetraacetic acid (EDTA) and 1 M NaCl (pH 8.0). DNA hybridization buffer was a phosphate buffer saline (PBS, pH 7.0) solution prepared by 10 mM NaH_2PO_4-Na_2HPO_4 and 1 M NaCl. DNA-Au bio-bar codes stock buffer was 10 mM PBS solution (pH 7.0) containing 0.3 M NaCl. All solutions were prepared with Milli-Q water (18 MΩ·cm resistivity) from a Millipore system.

Table 1
Oligonucleotides used in the assay.

Synthetic oligonucleotides	Sequence (5′→3′)
Capture probe	NH_2-$(CH_2)_6$-CAC CTC TCT TTT ATC TGG TT
Signal probe 1 (S1)	GCT TCC TGA AGT GAG TAC TCTA A-$(CH_2)_6$-SH
Signal probe 2 (S2)	ATG GTA TTG CTA CGA TCA CT-SH
Target DNA	GAG TAC TCA CTT CAG GAA GCA ACC AGA TAA AAG AGA GGT G
Single-base mismatched DNA	GAG TAC TCA CTA CAG GAA GCA ACC AGA TAA AAG AGA GGT G
Non-complementary DNA	ATC ACG GTT GCA TCA TGT AGC GAG TTC CGT TCT TAG TCA T

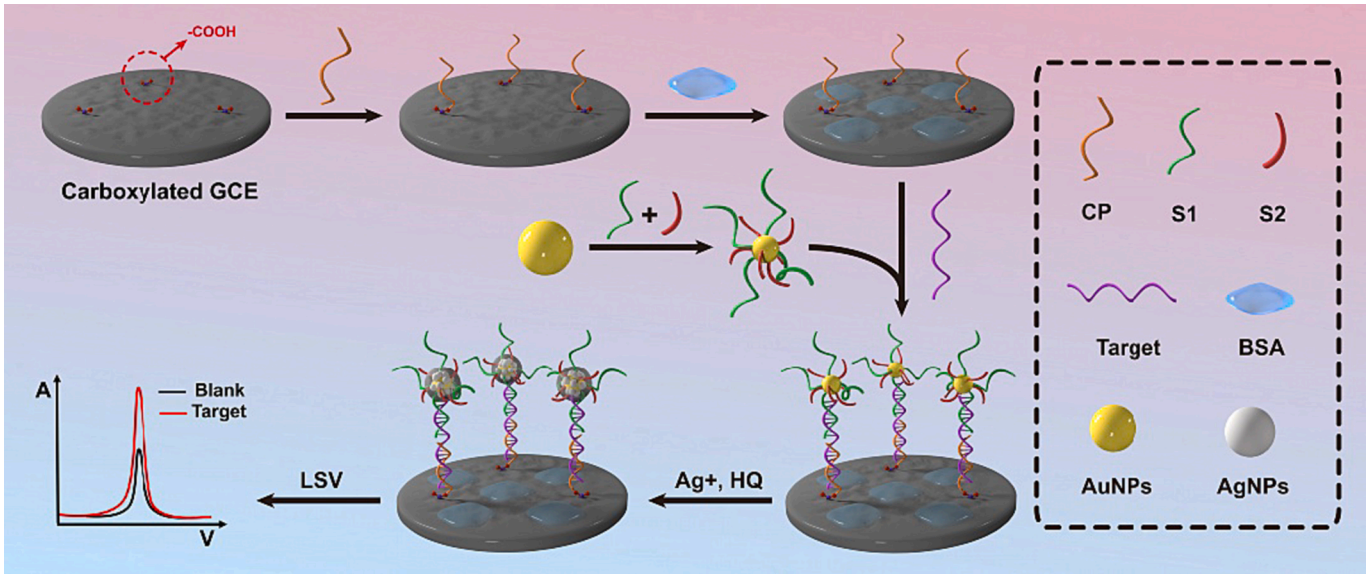

Scheme 1. Schematic diagram of the procedure for the fabrication of dual-amplification DNA biosensor. (A) Synthetic process of DNA-Au bio-bar codes. (B) Covalent bond of ssDNA on the carboxyl-functionalized /GCE and detection. DNA: deoxyribonucleic acid; ssDNA: single strand DNA; GCE: glassy carbon electrode.

Scanning electron microscope (SEM) images were carried out on a S-4800 scanning electron microscope (Hitachi, Japan). Ultraviolet–visible (UV–vis) absorption spectrum was acquired with an UV-2450 spectrophotometer (Shimadzu, Japan). Electrochemical experiment for linear sweep voltammetry (LSV) was carried on a CHI 630C electrochemical analyser (CH Instruments, China) equipped with a three-electrode system consisting of a GCE (3 mm in diameter) as working electrode, a platinum wire (counter electrode) and an Ag/AgCl electrode (3.0 M KCl, as reference electrode). The electrochemical impedance spectroscopy (EIS) measurement was performed on an Autolab PGSTAT30 electrochemical workstation (Metrohm, Netherlands).

2.2. Preparation of DNA-Au bio-bar codes

2.2.1. Preparation of AuNPs

AuNPs were synthesized via reduction of $HAuCl_4{\cdot}4H_2O$ by trisodium citrate and tannic acid [35]. The ratio of tannic acid to trisodium citrate determines the size and distribution of the synthesized AuNPs. Two initial aqueous solutions, including 1 mL of 2 wt% $HAuCl_4{\cdot}4H_2O$ solution diluted with 79 mL distilled water, and a mixture of 8 mL of 1 wt% trisodium citrate and 0.2 mL of 1 wt% tannic acid that was diluted with 11.8 mL distilled water, were respectively added in two round-bottom flasks and simultaneously heated to 60 °C. Then, the mixture was rapidly added to the former under rigorous stirring for 35 min to obtain AuNPs solution. The concentration of as-synthesized AuNPs was determined to be 0.12 mg mL^{-1} on the basis of the concentration of $HAuCl_4{\cdot}4H_2O$ before reaction, assuming a 100 % reduction yield of the $AuCl_4^-$ ions [36].

2.2.2. Preparation of DNA-Au bio-bar codes

The process of signal probe 1 (S1) and signal probe (S2) labeling was performed according to references [37,38]. The mixture of 5×10^{-10} mol S1 and 2×10^{-9} mol S2 was activated with 1 mL of 10 mM phosphate buffer (PB) solution (pH 7.0) and 1.5 μL of 10 mM freshly prepared TCEP for 1 h, then added to 1 mL of AuNPs, and shaken gently overnight at room temperature to harvest original DNA-Au bio-bar codes. Afterwards, 1 mL of 10 mM PBS buffer solution (10 mM PB + 0.1 M NaCl, pH 7.0) was added into DNA-Au bio-bar codes for aging. Over the course of 40 h, excess reagents were removed by centrifuging at 14,000 rpm for 30 min. The red precipitate was rinsed and centrifuged for three times. The resulting nanoparticles were dispersed into the DNA-Au bio-bar codes stock buffer and stored at 4 °C.

2.3. Fabrication of electrochemical DNA biosensor with sandwich structure

Firstly, GCE was polished successively with 1, 0.3 and 0.05 μm Al_2O_3 slurry, and rinsed thoroughly with double-distilled water (DDW). Secondly, the electrode was sonicated in 50 % nitric acid (volume ration of DDW *vs.* HNO_3 = 1:1), acetone and DDW for 3 min in order, and allowed to dry at room temperature. Thirdly, the clean GCE was oxidized at the constant potential of +0.5 V in 10 mM PBS solution (pH 7.4) for 60 s, cleaned with DDW and dried with nitrogen. Fourthly, the pre-treated GCE was immersed into 200 μL of 10 mM PBS solution (pH 7.4) involving 5 mM EDC and 8 mM NHS for 30 min. Subsequently, the activated electrode was washed with DDW and dried with nitrogen to obtain a carboxy-functionalized GCE. Fifthly, 8 μL of 1×10^{-6} M capture probe was dropped on the GCE surface for 2 h at room temperature, followed by washing with DDW and air dry to obtain single strand DNA/GCE (ssDNA/GCE). Sixthly, the obtained electrode was immersed into 100 μL of 1 % bovine serum albumin (BSA) solution for 0.5 h to block possible remaining active sites against nonspecific adsorption, followed by thoroughly washing with DDW to remove non-specific binding probe. Seventhly, for the hybridization reaction, ssDNA/GCE was immersed into 100 μL of 10 mM PBS (pH 7.4) solution containing DNA-Au bio-bar codes and target DNA at 37 °C for 1 h, rinsed extensively with PBS solution and dried with nitrogen to obtain double strand DNA/GCE (dsDNA/GCE). Finally, under the action of reductant HQ, the silver ions were reduced to AgNPs on the surface of AuNPs to achieve signal amplification.

2.4. Electrochemical measurement

To get rid of oxygen from solution, nitrogen was aerated into the electrolyte solution before electrochemical measurement. EIS measurements were performed in 5 mM $[Fe(CN)_6]^{4-/3-}$ solution containing 0.1 M KCl at an open potential of 210 mV within the frequency range of 0.01 Hz to 100 kHz. And the amplitude of the applied sine wave potential was 5 mV. For LSV measurement, silver deposition enhancement solution was freshly prepared using a 200 μL mixture of silver enhancer A and B (obtained from silver enhancer kit, volume ration of A *vs.* B = 1:1) and stored in a dark incubator. The dsDNA/GCE was immersed into silver deposition enhancement solution for 8 min, washed and dried. Then LSV measurement was carried out in 1 M KCl solution (potential range: −0.1 – 0.2 V, scanning speed: 100 mV s^{-1}).

3. Results and discussion

3.1. Characterization of DNA-Au bio-bar codes

UV–vis spectroscopy had been firstly employed to monitor the interaction between AuNPs and DNA. As shown in Fig. 1C, the spectrum of AuNPs showed a characteristic absorption peak at 520 nm (curve a), which was characteristic of 16 nm spherical AuNPs [39,40]. The spectrum of DNA showed a characteristic absorption peak at 260 nm (curve b), and the spectrum of DNA-Au bio-bar codes displayed two absorption peaks around 260 nm and 523 nm (curve c). In comparison with AuNPs, red shift at 523 nm (curve c) provided evidence on the interaction between AuNPs and DNA molecules via Au-S bond, this phenomenon was consistent with the reported literature [41]. Further, we studied the stability of DNA-Au bio-bar codes by UV–vis spectroscopy. As shown in inset of Fig. 1C, the position of absorption peaks had no obvious change after 4 months and still remained two remarkable absorption peaks, indicating the stability of DNA-Au bio-bar codes.

3.2. Morphological characterization of the electrochemical DNA biosensor

The surface morphology of the modified electrode after silver deposited was characterized by SEM technique. In Fig. 1A, there were a great amount of spheroidal particles on GCE surface, indicating DNA-Au bio-bar codes were loaded on electrodes through sandwich-type hybridization. In Fig. 1B, brighter and bigger particles generated, because the AuNPs of DNA-Au bio-bar codes catalyzed silver ions deposition on electrodes to form AgNPs by HQ reduction. Due to probe S1 and probe S2 loading on AuNPs randomly, each of DNA-Au bio-bar codes catalytic ability were varying, which may cause a difference between the diameters of the particles, phenomenon similar with other related fields [42].

3.3. Electrochemical characterization of the electrochemical DNA biosensor

It is well known that EIS is an excellent technique for investigating the changes of interfacial properties of modified electrodes for each modification process. Fig. 1D showed the impedance spectra corresponding to the stepwise modification processes of the DNA biosensor. The EIS of the bare GCE exhibited almost a straight line that was characteristic of a diffusion limiting step of the electrochemical process (Fig. 1D, curve a). After functionalized with carboxyl group, the electron transfer resistance (R_{et}) increased to 375 Ω (carboxyl-functionalized GCE, curve b), due to the negative charge on electrode surface that

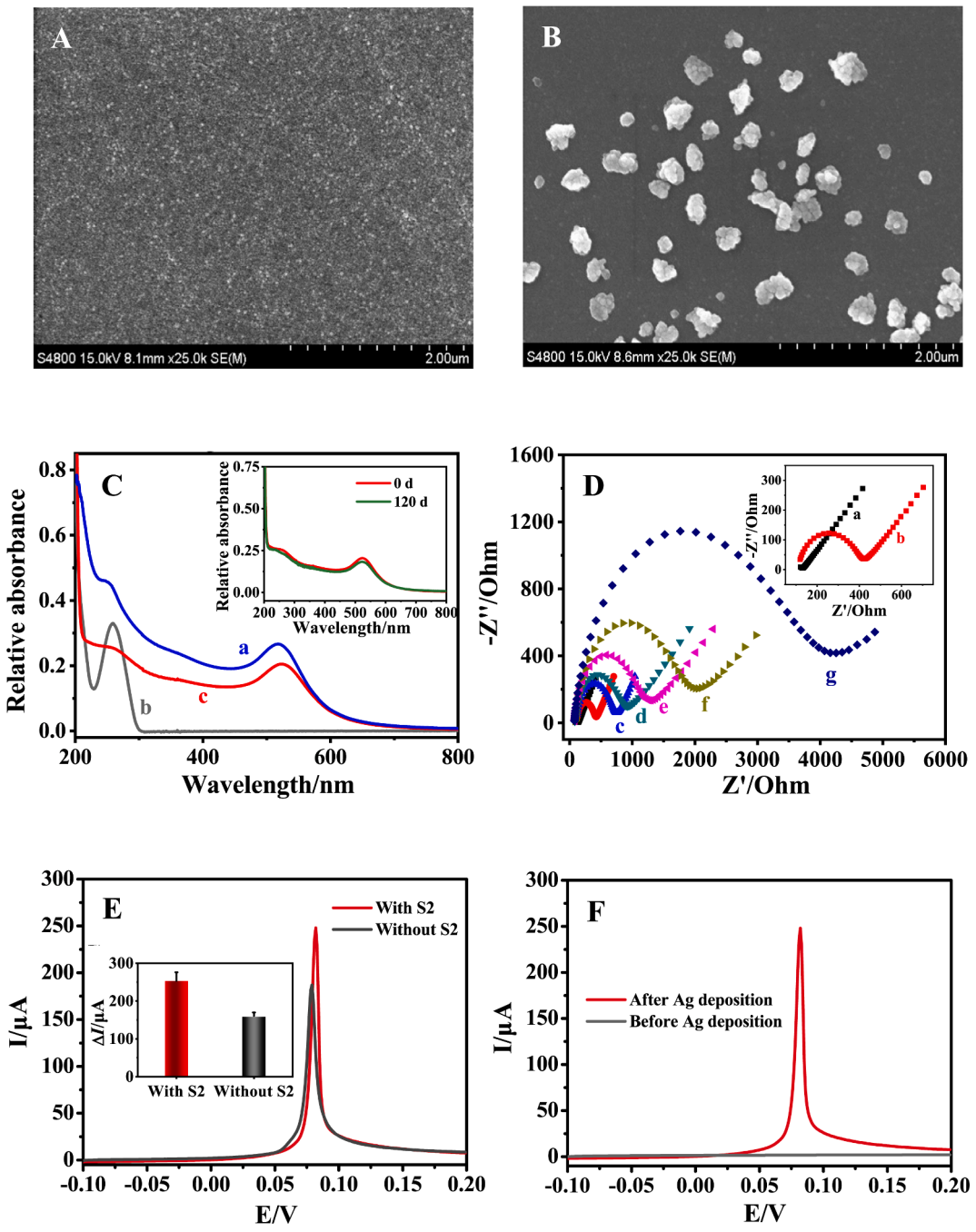

Fig. 1. SEM images of the electrode after sandwich-type hybridization (A) and after silver deposition (B).. (C) UV–vis spectra of AuNPs (curve a), DNA (curve b) and DNA-Au bio-bar codes (curve c). Inset: UV–vis spectra of DNA-Au bio-bar codes before and after 120 days. (D) EIS of bare GCE (a), carboxyl-functionalized GCE (b), activated GCE (c), ssDNA/GCE (d), BSA/ssDNA/GCE (e), dsDNA/GCE (f) and AgNPs/dsDNA/GCE (g). (E) LSV curves and signal histogram (inset) of AuNPs-DNA composites with and without S2. (F) LSV curves before and after silver disposition. SEM: Scanning electron microscope; UV–vis: Ultraviolet–visible; EIS: electrochemical impedance spectroscopy; BSA: bovine serum albumin; dsDNA: double strand DNA; LSV: linear sweep voltammetry; AuNPs: gold nanoparticles; AgNPs: silver nanoparticles.

hindered electric transmission between $[Fe(CN)_6]^{3-/4-}$ and electrode surface. After EDC/NHS activation, the resistance value slightly enhanced (curve c, 648 Ω, activated GCE). The R_{et} increased to 1002 Ω while capture probe was immobilized (curve d, 1002 Ω, ssDNA/GCE), because the negatively charged phosphate backbone of the probe DNA immobilized on the electrode repelled $[Fe(CN)_6]^{3-/4-}$. The R_{et} value further improved after the electrode was blocked with BSA (curve e, 1346 Ω, BSA/ssDNA/GCE). The prepared DNA biosensor was incubated with target DNA and DNA-Au bio-bar codes solution, and the formed sandwich-type complex on the electrode would further hinder the access of the redox probe to the electrode, causing a further increase in R_{et} (curve f, 2061 Ω, dsDNA/GCE). After silver enhancement on AuNPs surface, the resistance value was enlarged to 4173 Ω of curve g, which was caused by steric hindrance (AgNPs/dsDNA/GCE). The above results demonstrated the electrochemical DNA biosensor had been successfully prepared.

3.4. Dual signal amplification investigation

3.4.1. Dna-au bio-bar codes amplification experiment

AuNPs labeled DNA can realize signal amplification, researchers usually label DNA sequence on AuNPs as reporter DNA. Herein, we fixed two kinds of DNA sequences on AuNPs as reporter DNA. S1 was complementary with the target DNA, while the other S2 was not. The developed DNA-Au bio-bar codes were expected to amplify the current signal. There fall into two reasons, one is the length of S2 shorter than S1, so it can reduce space steric hindrance in the process of S1 combined with target DNA effectively; additionally one kind is the concentration of S2 higher than S1, it can dilute the density of S1 on AuNPs, taking more DNA-AuNPs compounds to electrode by chain reaction with target DNA compared with traditional DNA-AuNPs. In Fig. 1E, during the linear potential sweep process, the peak current of DNA-Au bio-bar codes coupled with biosensor was higher than the traditional DNA-AuNPs coupled counterpart, demonstrating signal amplification effect of DNA-Au bio-bar codes.

3.4.2. Silver enhancement characterization

Deposition of AgNPs on AuNPs was a convenient and label-free approach to prepare biosensor, and the signal was significantly increased. In this study, the electrochemical signal change before and after silver deposition was studied by LSV measurement. As shown in Fig. 1F, without silver deposition, the electrochemical DNA biosensor after hybridization exhibited no obvious oxidation peak (curve a). After reduction of Ag^{+}, the current emerged a distinct peak at + 0.08 V (curve b). The results showed that electrochemical signal was significantly enlarged after silver deposition. Hence, the silver deposition technology can greatly amplify the performance of the sensor.

3.5. Optimization of experimental conditions

The assay conditions can affect the hybridization efficiency of electrochemical DNA biosensor. The factors such as silver deposition time, DNA hybridization time and hybridization temperature were investigated. Firstly, we studied the effect of silver deposition time on response signal. The amount of AgNPs generation was affected by the action time of the silver enhancer solution on the AuNPs modified electrode. AuNPs were casted on GCE and dried at room temperature, then AuNPs/GCE was immersed into the freshly prepared silver enhancer solution, and the deposition time (5, 6, 7, 8, 9 and 10 min) was evaluated. As shown in Fig. 2A, the maximum response signal was observed at 8 min. Therefore, 8 min was used for silver deposition time in following experiments. Secondly, the effect of hybridization time among capture probe, DNA-Au bio-bar codes and target DNA (10 nM) at different time (30, 45, 60, 75 and 90 min) on detection signal was investigated. As shown in Fig. 2B, the response signal increased significantly as the hybridization time increased from 30 to 60 min, and tended to be stable after 60 min, indicating that the hybridization reaction was completed after 60 min. Hence, we selected 60 min as the optimum DNA hybridization time among capture/signal/target sequences. Thirdly, the effect of hybridization temperature was also examined (30, 32, 35, 37, 40, 42, 45 and 50 °C). As presented in Fig. 2C, the current response of the biosensor after hybridization increased with temperature up to 37 °C. However, the response decreased as the temperatures over 37 °C. Therefore, 37 °C was chosen in this study.

3.6. Analytical performance investigation

Under the optimal conditions, the analytical performance of the DNA biosensor based on DNA-Au bio-bar codes and AuNPs promoted reduction of silver ions was investigated. As shown in Fig. 3A, the peak current obtained after the hybridization reaction showed an increase with the increment of target DNA concentration, because the more DNA-Au bio-bar codes in hybridization solution, the more AgNPs generated, so LSV responses increased. The current value after deduction of the blank group (ΔI) was linear with the base-10 logarithm of the target DNA

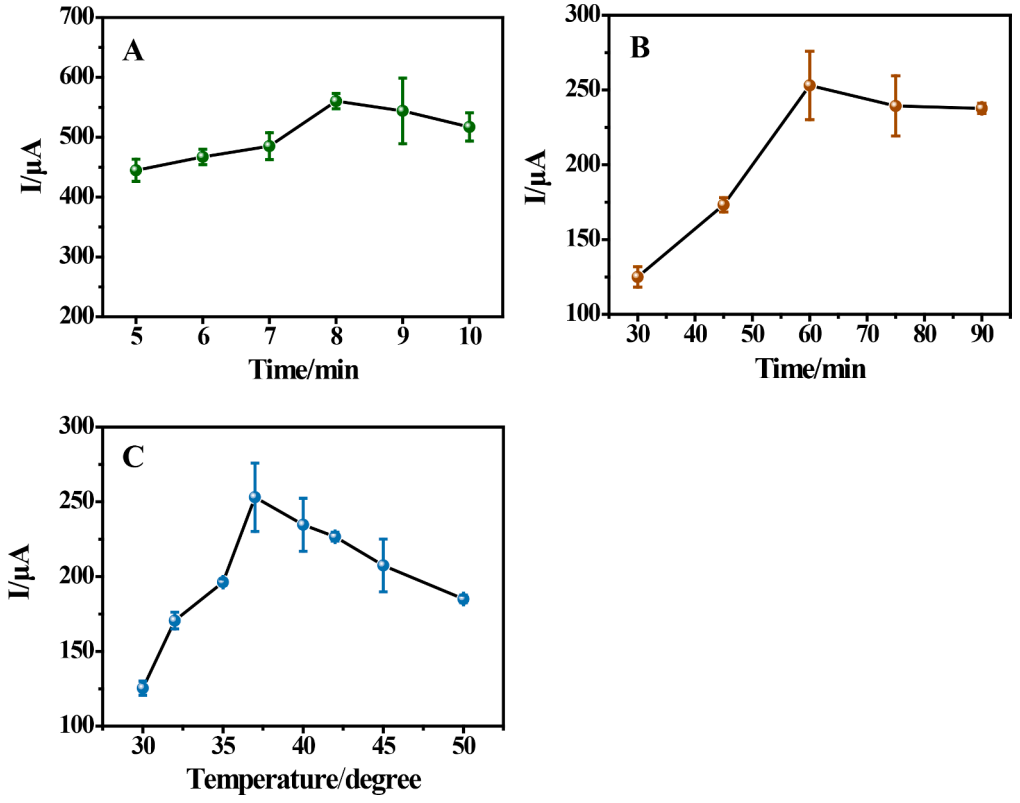

Fig. 2. Effects of silver deposition time (A), hybridization time (B) and hybridization temperature (C) on the peak current.

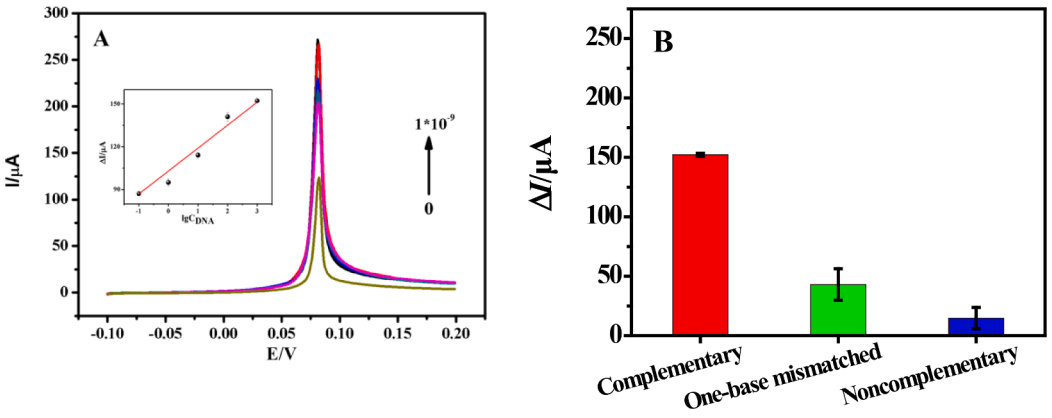

Fig. 3. (A) LSV curves of the electrochemical DNA biosensor towards target DNA at different concentrations, from down to top (black arrow): 0, 0.1, 1, 10, 100 and 1000 pM. Inset: Base-10 logarithmic plot of current versus the target DNA concentrations. (B) Δ*I* intensity of complementary DNA, one-base mismatched DNA and non-complementary DNA.

concentration (lgC_{DNA}) in the range from 100 fM to 1 nM. The blank group referred to the current signal without addition of target DNA, and other conditions remained the same. The linear regression equation was ΔI (μA) = 103 + 16.11 × lgC_{DNA} (pM), R^2 = 0.996, and the limit of detection (LOD) was 33 fM (S/N = 3). The selectivity of the electrochemical DNA biosensor was studied using three kinds of DNA sequence including perfectly complementary targets, one-base mismatched strands and non-complementary strands, at a concentration of 1 nM, 10 nM, 10 nM respectively. In Fig. 3B, the completely complementary target DNA obtained the maximum current signal (ΔI = 152.2 ± 1.27 μA), while the one-base mismatched strand (ΔI = 43.0 ± 13.3 μA) and non-complementary strand (ΔI = 14.7 ± 9.0 μA) were respectively corresponded to 28.2 % and 9.7 % of the complementary target group. Of note, the biosensor equipped with dual signal amplification strategy exhibited an excellent single-based discrimination ability even though the concentrations of mismatched strands was one order of magnitude higher than perfectly complementary target. Further, to evaluate the reproducibility of the biosensor, five electrodes were prepared for the detection of 1 nM target DNA. The relative standard deviation (RSD) of the measurements for the five electrodes was 12.40 % (data not shown). The above results demonstrated the high performance of biosensor with excellent sensitivity, specificity and reproducibility. Meanwhile, compared with other counterparts (Table 2), the developed biosensor had low detection limit and wide linear range, manifesting its prospect in disease-related DNA detection.

Table 2
Comparison of various electrochemical biosensors for gene detection.

Electrode/Methods	Target	Linear range/ Expression level	Detection limit	Reference
AuNPs/toluidine blue-graphene oxide modified GCE	MDR1 gene	10 pM−1 nM	2.95 pM	[43]
AuNPs modified screen printed carbon electrode	*Citrus tristeza virus*-related gene	0.1 μM−10 μM	100 nM	[44]
Screen-printed gold nanostructured electrode	*Bacillus thuringiensis* related cry1 gene	1 μM−1 pM	997 fM	[45]
RT-qPCR	MDR1 gene	15–653 copies/mL	–	[8]
RT-qPCR	MDR1 gene	4.07–8.97 copies/mL	–	[46]
GCE coupled with dual signal amplification strategy	MDR1 gene	100 fM−1 nM	33 fM	This work

3.7. Recovery experiment

To verify the accuracy of the electrochemical DNA biosensor for detecting MDR1, acute leukemia gene were obtained and diluted to 10 nM with hybridization buffer. Afterwards, the standard solution of MDR1 gene was added and the recovery test was determined by the standard addition method using the established biosensor. In Table 3, a good recovery in the range of 92.6 % − 95.5 % was achieved. The result demonstrated the developed biosensor could accurately determine the MDR1 against interferents.

4. Conclusion

In summary, taking advantages of DNA-Au bio-bar codes and silver enhancement effect, an electrochemical DNA biosensor was established for ultrasensitive determination of MDR1 gene without the need for target amplification. On the one hand, DNA-Au bio-bar codes could improve the efficiency of DNA hybridization via facilitating signal probe enrichment on electrode and reducing the cross reaction between the target and reporter DNA. On the other hand, silver deposited on AuNPs offered a dramatic enhancement of the hybridization signal. Under the optimal conditions, the current signal was proportional to the base-10 logarithm of target DNA concentration in a wide range from 100 fM to 1 nM with a detection limit as low as 33 fM (S/N = 3), and the developed biosensor could distinguish the target sequence from single-base mismatched sequence. Therefore, given the high sensitivity, excellent specificity and good accuracy, the electrochemical DNA biosensor coupled with dual amplification tactic is a facile and alternative platform for disease-related gene detection of MDR1 gene and drug resistance progression in clinical research.

CRediT authorship contribution statement

Yan Hu: Investigation, Writing – original draft. **Quan-Yu Liu:** Writing – original draft. **Xi Lin:** Writing – original draft. **Xin-Hua Lin:** Project administration, Supervision, Writing – review & editing. **Hua-**

Table 3
Recovery results in acute leukemia samples (n = 3).

Sample number	Added (pM)	Mean value (pM)	RSD (%)	Recovery (%)
1	10	9.26	8.81	92.60
2	100	94.40	5.13	94.40
3	1000	955.30	2.31	95.53

Ping Peng: Project administration, Writing – review & editing. **Ai-Lin Liu:** Project administration, Supervision, Writing – review & editing.

Declaration of competing interest

The authors declare that they have no known competing financial interests or personal relationships that could have appeared to influence the work reported in this paper.

Data availability

No data was used for the research described in the article.

Acknowledgments

The authors gratefully acknowledge the financial support of the Foundation of Fujian Provincial Department of Education (JAT220085).

References

[1] R.C. Siegel, K.D. Miller, H.E. Fuchs, A. Jemal, Cancer statistics, CA. Cancer. J. Clin. 72 (2022) 7–33.
[2] M. Li, K. Liao, I.W. Pan, Y.T. Shih, Growing financial burden from high-cost targeted oral anticancer medicines among medicare beneficiaries with cancer, JCO. Oncol. Pract. 18 (2022) e1739–e1749.
[3] M.Z. Heydarabad, M. Nikasa, M. Vatanmakanian, A. Azimi, M.F. Hagh, Regulatory effect of resveratrol and prednisolone on MDR1 gene expression in acute lymphoblastic leukemia cell line (CCRF-CEM): an epigenetic perspective, J. Cell. Biochem. 119 (2018) 4890–4896.
[4] D.G. Dastidar, D. Ghosh, A. Das, Recent developments in nanocarriers for cancer chemotherapy, OpenNano. 18 (2022) 100080.
[5] T. Haider, V. Pandey, N. Banjare, P.N. Gupta, V. Soni, Drug resistance in cancer: mechanisms and tackling strategies, Pharmacol. Rep. 72 (2020) 1125–1151.
[6] N.G. Jha, D.S. Dkhar, S.K. Singh, S.J. Malode, N.P. Shetti, P. Chandra, Engineered biosensors for diagnosing multidrug resistance in microbial and malignant cells, Biosensors 13 (2023) 235.
[7] M. Schaich, T. Illmer, Mdr1 gene expression and mutations in ras proto-oncogenes in acute myeloid leukemia, Leuk. Lymphoma. 43 (2022) 1345–1354.
[8] A. Haque, K.H.W. Sait, Q. Alam, M.Z. Alam, N. Anfinan, A.W.N. Wali, M. Rasool, MDR1 gene polymorphisms and its association with expression as a clinical relevance in terms of response to chemotherapy and prognosis in ovarian cancer, Front. Genet. 11 (2020) 516.
[9] M.M. Gottesman, I.H. Pastan, The role of multidrug resistance efflux pumps in cancer: Revisiting a JNCI publication exploring expression of the MDR1 (P-glycoprotein) gene, J. Nat. Cancer. Inst. 107 (2015) djv222.
[10] A. Lomae, P. Preechakasedkit, O. Hanpanich, T. Ozer, C.S. Henry, A. Maruyama, E. Pasomsub, A. Phuphuakrat, S. Rengpipat, T. Vilaivan, O. Chailapakul, N. Ruecha, N. Ngamrojanavanich, Label free electrochemical DNA biosensor for COVID-19 diagnosis, Talanta 253 (2023) 123992.
[11] Q. Liang, Y. Huang, M. Wang, D. Kuang, J. Yang, Y. Yi, H. Shi, J. Li, J. Yang, G. Li, An electrochemical biosensor for SARS-CoV-2 detection via its papain-like cysteine protease and the protease inhibitor screening, Chem. Eng. J. 452 (2023) 139646.
[12] W. Fu, H. Wang, C. Wang, L. Mei, X. Lin, X. Han, S. Zhu, A high-throughput liquid bead array-based screening technology for Bt presence in GMO manipulation, Biosens. Bioelectron. 77 (2016) 702–708.
[13] C.L. Manzanares-Palenzuela, B. Martín-Fernández, M. Sánchez-Paniagua López, B. López-Ruiz, Electrochemical genosensors as innovative tools for detection of genetically modified organisms, Trac-Trend, Anal. Chem. 66 (2015) 19–31.
[14] R.Z.A. Raja Jamaluddin, L.L. Tan, K.F. Chong, L.Y. Heng, An electrochemical DNA biosensor fabricated from graphene decorated with graphitic nanospheres, Nanotechnology 31 (2020) 485501.
[15] Q. Liu, H. Xie, J. Liu, J. Kong, X. Zhang, A novel electrochemical biosensor for lung cancer-related gene detection based on copper ferrite-enhanced photoinitiated chain growth amplification, Anal. Chim. Acta 1179 (2021) 338843.
[16] A. Majid, S. Mona, H. Shiva, Label-free electrochemical DNA biosensor for guanine and adenine by ds-DNA/poly(L-cysteine)/Fe3O4 nanoparticles-graphene oxide nanocomposite modified electrode, Biosens. Bioelectron. 102 (2021) 70–79.
[17] F. Liu, K. Li, Y. Zhang, J. Ding, T. Wen, X. Pei, Y. Yan, W. Ji, J. Liu, X. Zhang, L. Li, An electrochemical DNA biosensor based on nitrogen-doped graphene nanosheets decorated with gold nanoparticles for genetically modified maize detection, Microchim. Acta 187 (2020) 574.
[18] Y. Jiang, S. Li, P. Zhu, J. Zhao, X. Xiong, Y. Wu, X. Zhang, Y. Li, T. Song, W. Xiao, Z. Wang, J. Han, Electrochemical DNA biosensors based on the intrinsic topological insulator $BiSbTeSe_2$ for potential application in HIV determination, ACS Appl. Bio. Mater. 5 (2022) 1084–1091.
[19] Z. Zhang, P. Sen, B.R. Adhikari, Y. Li, L. Soleymani, Development of nucleic acid-based electrochemical biosensors for clinical applications, Angew. Chem. Int. Edit. 61 (2022) e202212496.
[20] H. Yang, Y. Xu, Q. Hou, Q. Xu, C. Ding, Magnetic antifouling material based ratiometric electrochemical biosensor for the accurate detection of CEA in clinical serum, Biosens. Bioelectron. 208 (2022) 114216.
[21] B.L. Littleford-Colquhoun, V.I. Sackett, C.V. Tulloss, T.R. Kartzinel, Evidence-based strategies to navigate complexity in dietary DNA metabarcoding: a reply, Mol. Ecol. 31 (2022) 5660–5665.
[22] X. Zhang, H. Zhi, F. Wang, M. Zhu, H. Meng, P. Wan, L. Feng, Target-Responsive smart nanomaterials via a Au-S binding encapsulation strategy for electrochemical/colorimetric dual-mode paper-based analytical devices, Anal. Chem. 94 (2022) 2569–2577.
[23] Y. Xu, X. Wang, C. Ding, X. Luo, Ratiometric Antifouling Electrochemical biosensors based on multifunctional peptides and MXene loaded with Au nanoparticles and methylene blue, ACS. Appl. Mater, Interfaces 13 (2021) 20388–20396.
[24] M. D'Acunto, P. Cioni, E. Gabellieri, G. Presciuttini, Exploiting gold nanoparticles for diagnosis and cancer treatments, Nanotechnology 32 (2021) 192001.
[25] Y. Ma, Y. Zhao, X. Xu, S. Ding, Y. Li, Magnetic covalent organic framework immobilized gold nanoparticles with high-efficiency catalytic performance for chemiluminescent detection of pesticide triazophos, Talanta 235 (2021) 122798.
[26] X. Zhang, Y. Ge, M. Liu, Y. Pei, P. He, W. Song, S. Zhang, DNA-Au Janus nanoparticles for in situ SERS detection and targeted chemo-photodynamic synergistic therapy, Anal. Chem. 94 (2022) 7823–7832.
[27] H.D. Hill, R.A. Vega, C.A. Mirkin, Nonenzymatic detection of bacterial genomic DNA using the bio bar code assay, Anal. Chem. 79 (2007) 9218–9223.
[28] J.M. Nam, C.S. Thaxton, C.A. Mirkin, Nanoparticle-based bio-bar codes for the ultrasensitive detection of proteins, Science 301 (2003) 1884–1886.
[29] L. Wang, J. Song, X. Wang, H. Qi, Q. Gao, C. Zhang, Monitoring casein kinase II at subcellular level via bio-bar-code-based electrochemiluminescence biosensing method, Chin. Chem. Lett. 31 (2020) 2520–2524.
[30] K. Zhang, S. Lv, Z. Lin, M. Li, D. Tang, Bio-bar-code-based photoelectrochemical immunoassay for sensitive detection of prostate-specific antigen using rolling circle amplification and enzymatic biocatalytic precipitation, Biosens. Bioelectron. 101 (2018) 159–166.
[31] K. Hu, D. Lan, X. Li, S. Zhang, Electrochemical DNA biosensor based on nanoporous gold electrode and multifunctional encoded DNA-Au bio bar codes, Anal. Chem. 80 (2008) 9124–9130.
[32] X. Zhou, P. Li, X. Wu, X. Lin, L. Zhao, H. Huang, J. Wu, H. Cai, M. Xu, H. Zhou, P. Sun, Multifunctional biosensor constructed by Ag-coating magnetic-assisted unique urchin core porous shell structure for dual SERS enhancement, enrichment, and quantitative detection of multi-components inflammatory markers, Biosens. Bioelectron. 210 (2022) 114257.
[33] Y. Gan, M. Zhou, H. Ma, J. Gong, S.Y. Fung, X. Huang, H. Yang, Silver nano-reporter enables simple and ultrasensitive profiling of microRNAs on a nanoflower-like microelectrode array on glass, J. Nanobiotechnology 20 (2022) 456.
[34] L. Ding, R. Qian, Y. Xue, W. Cheng, H. Ju, In situ scanometric assay of cell surface carbohydrate by glyconanoparticle-aggregation-regulated silver enhancement, Anal. Chem. 82 (2010) 5804–5809.
[35] T. Siebrands, M. Giersig, P. Mulvaney, C. Fischer, Steric exclusion chromatography of nanometer-sized gold particles, Langmuir 9 (1993) 2297–2300.
[36] M. Hu, Y. Yamaguchi, T. Okubo, Self-assembly of waterdispersed gold nanoparticles stabilized by a thiolated glycol derivative, J. Nanopart. Res. 7 (2005) 187–193.
[37] L.J. Ou, P.Y. Jin, X. Chu, J.H. Jiang, R.Q. Yu, Sensitive and visual detection of sequence-specific DNA-binding protein via a gold nanoparticle-based colorimetric biosensor, Anal. Chem. 82 (2010) 6015–6024.
[38] W. Zhao, L. Lin, I.-M. Hsing, Rapid synthesis of DNA-functionalized gold nanoparticles in salt solution using mononucleotide-mediated conjugation, Bioconjug. Chem. 20 (2009) 1218–1222.
[39] X. Liu, Y. Zhao, Y. Ding, J. Wang, J. Liu, Stabilization of gold nanoparticles by hairpin DNA and implications for label-free colorimetric biosensors, Langmuir 38 (2022) 5542–5549.
[40] Q. Li, F. Liu, C. Lu, J.M. Lin, Aminothiols sensing based on fluorosurfactant-mediated triangular gold nanoparticle-catalyzed luminol chemiluminescence, J. Phys. Chem. c. 115 (2011) 10964–10970.
[41] J. Choi, H. Kim, J. Choi, J. Choi, B. Oh, Signal enhancement of silicon nanowire-based biosensor for detection of matrix metalloproteinase-2 using DNA-Au nanoparticle complexes, ACS Appl. Bio. Mater. 5 (2013) 12023–12028.
[42] N. Jaffrezic-Renault, C. Martelet, Y. Chevolot, Biosensors and bio-Bar code assays based on biofunctionalized magnetic microbeads, Sensors 4 (2008) 589–614.
[43] H.P. Peng, Y. Hu, P. Liu, Y.N. Deng, P. Wang, W. Chen, A.L. Liu, Y.Z. Chen, X. H. Lin, Label-free electrochemical DNA biosensor for rapid detection of mutidrug resistance gene based on Au nanoparticles/toluidine blue-graphene oxide nanocomposites, Sensor. Actuat. B-Chem. 207 (2015) 269–276.
[44] M. Khater, A. Escosura-Muñiz, D. Quesada-González, A. Merkoçi, Electrochemical detection of plant virus using gold nanoparticle-modified electrodes, Anal. Chim. Acta 1046 (2019) 123–131.
[45] V. Raju, V. Bhavana, G. Gayathri, S. Suryan, R. Reddy, N. Reddy, C. Ravikumar, M. Santosh, A novel disposable electrochemical DNA biosensor for the rapid detection of Bacillus thuringiensis, Microchem. J. 159 (2020) 105434.
[46] I. Gramer, M. Kessler, J. Geyer, Determination of MDR1 gene expression for prediction of chemotherapy tolerance and treatment outcome in dogs with lymphoma, Vet. Comp. Oncol. 13 (2015) 363–372.